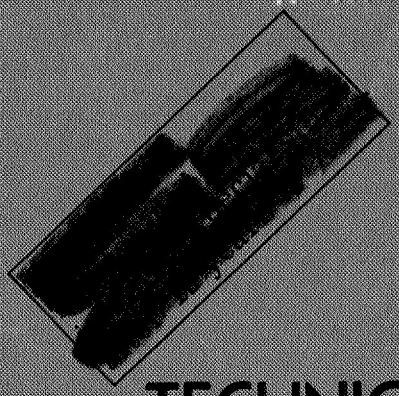

TECHNICAL MEMORANDUM

X-733

STATIC LONGITUDINAL AERODYNAMIC CHARACTERISTICS AT A MACH NUMBER OF 10.03 OF LOW-ASPECT-RATIO WING-BODY CONFIGURATIONS SUITABLE FOR REENTRY

By Lawrence E. Putnam and Cuyler W. Brooks, Jr.

Langley Research Center
Langley Station, Hampton, Va.

NATIONAL AERONAUTICS AND SPACE ADMINISTRATION
WASHINGTON
December 1962

NATIONAL AERONAUTICS AND SPACE ADMINISTRATION

TECHNICAL MEMORANDUM X-733

STATIC LONGITUDINAL AERODYNAMIC CHARACTERISTICS AT A MACH NUMBER OF 10.03 OF LOW-ASPECT-RATIO WING-BODY CONFIGURATIONS SUITABLE FOR REENTRY*

By Lawrence E. Putnam and Cuyler W. Brooks, Jr.

SUMMARY

An investigation has been made in the Langley 15-inch hypersonic flow apparatus to study the effect of wing planform geometry on the static longitudinal aerodynamic characteristics of low-aspect-ratio wing-body configurations. This investigation also included a study of the effects of wing leading-edge shape and wing lower-surface contour on the longitudinal characteristics of several of these configurations. The results were obtained at a Mach number of 10.03 and at angles of attack from about -4° to 42°. The Reynolds number, based on the wing mean aerodynamic chord, varied from about 0.41×10^6 to 0.58×10^6.

In general the circular planform model and the 65° triangular flat-plate model developed the highest lift coefficients and the 75° (clipped) flat-plate model developed the lowest lift coefficient throughout the angle-of-attack range of the present investigation. The circular model had the highest drag coefficient and the 75° clipped model had the lowest value of drag coefficient of the flat-plate wing models. Maximum lift-drag ratio for the flat-plate models varied from 2.3 for the 75° triangular configuration to 1.8 for the circular configuration. All the flat-plate models were unstable about the wing centroid of area. Changing from a semicylindrical to a square wing leading edge on the 65° triangular wing configuration had essentially no effect on lift coefficient but caused higher drag, lower lift-drag ratio, and only small changes in stability. Contouring the lower surface of the elliptical planform wing caused a large decrease in stability and a reduction in maximum lift-drag ratio from 2.0 to 1.4. The trihedron model had higher drag coefficient and lower maximum lift-drag ratio than the 75° triangular flat-plate model. The trihedron model was the only stable configuration for the moment reference center of the present investigation.

*Title, Unclassified.

INTRODUCTION

At the present time there is an intense interest in vehicles suitable for reentry into the earth's atmosphere. Such problems as reentry heating, lateral and longitudinal range control, and g-loading are all dependent on the aerodynamic characteristics of the reentry vehicle. The two main categories of vehicles under consideration for reentry are the ballistic and the lifting types. The ballistic vehicle is perhaps the simplest solution to the reentry problem, but this type has numerous undesirable features. The lifting vehicle, which includes lifting body and winged configurations, allows reduction of the gravity forces associated with reentry and a large increase in lateral and longitudinal range.

The National Aeronautics and Space Administration has made a number of investigations on winged reentry vehicles. (For example, see refs. 1 to 6.) The longitudinal aerodynamic characteristics of several winged configurations similar to those of the present investigation at supersonic speeds are available in references 1 and 2.

The purpose of the present investigation is to show the effects of wing planform on the static longitudinal aerodynamic characteristics at hypersonic speeds for several low-aspect-ratio wing-body configurations. The test results were obtained on configurations with six different wing planforms. Wing leading-edge shape and wing lower-surface contour were also varied in the investigation. The investigation was made in the Langley 15-inch hypersonic flow apparatus at a Mach number of 10.03. The angle of attack ranged from about -4° to 42°.

SYMBOLS

The forces and moments are referenced to the stability axes which have their origin at the centroid of area of the model planforms and on the center line of the model fuselage. The angle of attack is referenced to the flat upper surface of each wing.

A	aspect ratio
c	local chord
$\bar{c}$	mean aerodynamic chord
C_D	drag coefficient, $\frac{\text{Drag}}{qS}$
C_L	lift coefficient, $\frac{\text{Lift}}{qS}$
C_m	pitching-moment coefficient, $\frac{\text{Pitching moment}}{qS\bar{c}}$

C_{L_α}	lift-curve slope per degree at zero angle of attack, $\left(\frac{\partial C_L}{\partial \alpha}\right)_{\alpha=0^\circ}$
d	diameter
l	length
L/D	lift-drag ratio
$(L/D)_{max}$	maximum lift-drag ratio
M	Mach number
q	free-stream dynamic pressure
r	radius
R	Reynolds number based on mean aerodynamic chord
S	wing area
y	distance from tunnel horizontal center line
α	angle of attack, deg
$\alpha_{(L/D)max}$	angle of attack for $(L/D)_{max}$, deg
λ	taper ratio, $\frac{\text{Tip chord}}{\text{Root chord}}$

MODELS

A drawing of a typical model-sting arrangement is shown in figure 1 and a photograph of the models is shown as figure 2. Figure 3 gives details of the six basic flat-plate models and figure 4 presents drawings of the ellipse (convex) and trihedron models. Table I presents several additional geometric parameters for each configuration. The basic models had a flat-plate wing which was 0.183 inch thick with a semicylindrical leading edge. The semicylindrical leading edge had a radius of 0.092 inch normal to the wing leading edge. The wing trailing edge for all models was square. All the models were equipped with bodies having identical blunted half-conical noses and similar cylindrical afterbodies which varied in length with each model. (See fig. 3(b).) These cone-cylinder bodies were mounted on spacers on the wing upper surface. (See figs. 1 and 3(b).) The wing planforms of the six basic models were a circle, an ellipse, a 65° swept delta, a 65° swept clipped-tip delta (λ = 0.284), a 75° swept delta, and a 75° swept clipped-tip delta (λ = 0.300). (See fig. 3(a).)

In addition to the six basic models, a 65° swept delta flat-plate wing model with a square wing leading edge and an ellipse model (fig. 4(a)) with a contoured

wing lower surface were investigated. Also tested was a trihedron model which had a 75° swept right triangular pyramidal wing. The upper surface of the wing was flat and the lower surface had a dihedral angle of 45°. (See fig. 4(b).)

APPARATUS AND TESTS

Tunnel

The investigation was made in the Langley 15-inch hypersonic flow apparatus which is a Mach number 10.03 blowdown wind tunnel. (See fig. 5.) The tunnel has an axisymmetric contoured nozzle with a 15-inch-diameter test section. Tests are made at stagnation pressures up to 1,500 psia for air temperatures up to 1,500° F; a direct-current electrical resistance-tube heater provides sufficient temperature to avoid liquefaction of the air.

The tunnel air supply is stored in a 1,030-cu-ft tank farm at 1,800 psia; the air is initially dried to -60° F at 1,800 psia. The tunnel air is exhausted through an aftercooler to an 83,000-cu-ft vacuum tank that can be evacuated to about 0.20 psia.

Figure 6 shows typical Mach number distributions for various longitudinal stations in the test section of the hypersonic flow apparatus. The data shown in this figure were obtained from measurement of stagnation pressure. The unflagged data points were obtained by determining the Mach number from the ratio of stagnation pressures across a normal shock. At $y = \pm 4.5$ inches and at longitudinal stations 0, 4 inches aft, and 8 inches aft, calculating the Mach number from the ratio of stagnation pressures shows an increase in the Mach number, which indicates that the points are in the boundary layer. In order to get a more realistic value for the Mach numbers in the boundary layer, the data shown by the flagged symbols were obtained by assuming the static pressure to be constant through the boundary layer and using the ratio of static pressure to measured local stagnation pressure. These Mach number distributions shown in figure 6 indicate that the tunnel has a uniform core of air about 10 inches in diameter and at least 16 inches long.

On the basis of static-pressure data obtained on a wedge and of measured force data on symmetrical models, the flow inclination is indicated to be negligible.

Tests

Two different sting-supported internal six-component strain-gage balances were used in this test to provide maximum accuracy throughout the angle-of-attack range. One balance was used for the range from about -4° to 20° and the other from about 20° to 42°. The tests were made at a stagnation pressure of 800 psia and a stagnation temperature of 1,350° F, which corresponds to a Reynolds number per foot of 1.32×10^6. The Reynolds number, based on the mean aerodynamic chord, varied from 0.41×10^6 for the circle model to 0.58×10^6 for the ellipse model.

The angle of attack ranged from about -4° to 42°. Boundary-layer transition was natural for these tests.

Corrections

The angle of attack has been corrected for sting and balance deflections due to aerodynamic loads. The axial-force data have been adjusted to a condition of free-stream static pressure at the model fuselage base. The reference area for the base pressures was the base area of the model fuselage. (See fig. 3(b).) The change in axial-force coefficient associated with a change in base pressure from free stream to zero amounts to only 0.0009.

RESULTS AND DISCUSSION

Presentation of Results

The effect of planform variation on the longitudinal aerodynamic characteristics of the six basic flat-plate wing-body configurations is shown in figure 7. Figure 8 shows the effect of wing leading-edge shape on the longitudinal aerodynamic characteristics of the 65° triangular wing configuration. The effect of wing lower-surface contour on the longitudinal aerodynamic characteristics of the elliptical planform configuration is shown in figure 9 and a comparison of the longitudinal aerodynamic characteristics of the trihedron model with the 75° triangular configuration is presented in figure 10. Schlieren photographs of each configuration at several angles of attack are shown as figure 11. Table II presents a summary of lift-curve slope at $\alpha = 0^\circ$, maximum lift-drag ratio, and angle of attack for $(L/D)_{max}$ for all the models tested.

Effect of Planform Variation

Lift coefficient.- The effects of planform geometry on the variation of lift coefficient with angle of attack is shown in figure 7(a). Generally, the circle and 65° models develop the highest lift coefficient for a given angle of attack and the 75° (clipped) model has the lowest lift coefficient. The 65° model has the highest value of lift-curve slope at zero angle of attack (0.0090) and the 75° (clipped) model has the lowest value (0.0065).

Although increasing the wing sweep of the triangular wing from 65° to 75° causes a reduction in C_{L_α} from 0.0090 to 0.0066, increasing sweep has very little effect on lift coefficient at angles of attack up to approximately 18°. Increasing the wing sweep causes a decrease in lift coefficient above an angle of attack of approximately 18°. This decrease in lift coefficient probably results from the decreasing lower-wing-surface pressures due to a decrease in the strength of the shock-wave system with increasing sweep.

Although clipping the wing tips of the 65° model (planform area remaining essentially constant) causes a reduction in C_{L_α} from 0.0090 to 0.0075, clipping

the tips has very little effect on lift coefficient up to an angle of attack of about 18°. Above an angle of attack of 18°, clipping the wing tips of the 65° model results in a small decrease in lift coefficient. Clipping the wing tips of 75° configuration has essentially no effect on lift coefficient.

Changing the eccentricity of the circle planform to the ellipse planform causes a decrease in lift coefficient throughout the angle-of-attack range of the present investigation. This decrease in lift coefficient is associated with the reduction in strength of the bow-shock system on the ellipse model as compared with that on the circle model. This reduction resulted in lower pressures on the lower wing surface of the ellipse model. The circle model has a value of C_{L_α} of 0.0078 and the ellipse model has a value of C_{L_α} of 0.0072.

Drag coefficient.- Figure 7(b) shows the effect of planform geometry on drag coefficient. Generally, the circle model has the highest value of drag coefficient for a given angle of attack and the 75° (clipped) model has the lowest value of drag coefficient. The higher values of drag coefficient of the circle model are most likely due to the strong bow shock and corresponding wave drag associated with this model. Decreasing the sweep angle of the triangular wing from 75° to 65° results in a corresponding increase in drag coefficient for a given angle of attack due to the stronger shock system. Clipping the wing tips of the triangular configurations has essentially no effect on drag coefficient up to angles of attack of approximately 18°. At higher angles of attack, clipping the wing tips causes a decrease in drag coefficient.

Lift-drag ratio.- The effect of planform geometry on the variation of lift-drag ratio with angle of attack is shown in figure 7(c). As would be expected because of its high drag, the circle model has the lowest value of maximum lift-drag ratio (1.8), which occurs at an angle of attack of approximately 22°. The 75° model has the highest value of maximum lift-drag ratio (2.3), which occurs at an angle of attack of approximately 14°. Decreasing the sweep angle of the triangular wings to 65° causes a decrease in $(L/D)_{max}$ to 2.1. Clipping the tips of the 65° and 75° triangular models has essentially no effect on $(L/D)_{max}$.

Pitching-moment coefficient.- The effect of planform geometry on the variation of pitching-moment coefficient with angle of attack is shown in figure 7(d). All the flat-plate wing configurations are unstable in the angle-of-attack range of the present investigation (for the assumed centroid-of-area moment reference center), and the circle model is the most unstable. The large negative values of pitching-moment coefficient at zero angle of attack are associated with the positive pressures on the nose cone of the fuselage. The effect of these positive pressures on the pitching-moment coefficient diminishes as the angle of attack increases to about 18°. Above this angle of attack, the nose cone is shielded by the wing and it has a negligible effect on pitching-moment coefficient.

Effect of Wing Leading-Edge Shape

The effect of changing from a semicylindrical wing leading edge to a square wing leading edge on the 65° configuration is shown in figure 8. Although the square wing leading edge is not feasible due to heating considerations, it was

investigated to determine the sensitivity of the aerodynamic characteristics to leading-edge shape. The change in leading-edge shape has essentially no effect on lift coefficient, but generally causes an increase in the drag coefficient throughout the angle-of-attack range, as would be expected. This increased drag of the square leading edge results in lower values of lift-drag ratio below an angle of attack of about 37°. The values of maximum lift-drag ratio are 1.9 and 2.1 for the square- and cylindrical-leading-edge models, respectively.

The pitching-moment curves of figure 8 indicate that changing the shape of the wing leading edge from semicylindrical to square produces a negative increment in pitching-moment coefficient with little or no change in stability up to an angle of attack of approximately 28°. Above this angle of attack, the blunt (square) leading edge produces positive increments in pitching moment and a decrease in stability.

Effect of Wing Lower-Surface Shape

The effect of wing lower-surface shape on the longitudinal aerodynamic characteristics of the elliptical planform wing-body configuration is shown in figure 9. Contouring the lower surface increases the lift coefficient at angles of attack less than about 17° and decreases the lift coefficient at the higher values of α. The higher lift coefficients in the low angle-of-attack range (-4° to 17°) for the ellipse (convex) model are probably associated with the positive pressures on the forward section of the curved lower surface of the wing. At angles of attack greater than about 17°, the positive pressures acting on the wing lower surface are not as effective on the ellipse (convex) model as they are on the flat-bottom ellipse because of the chordwise and spanwise curvature of the contoured lower surface.

Contouring the wing lower surface of the ellipse model increases the drag coefficient at values of α less than about 34° because of the increase in wing thickness. At angles of attack greater than 34°, the ellipse (convex) model has the lower drag coefficient resulting from the reduction in drag due to lift associated with the previously noted lower lift developed in this angle-of-attack range. The values of maximum lift-drag ratio for the ellipse (convex) model and for the flat-plate ellipse model are 1.4 at an angle of attack of about 15° and 2.0 at an angle of attack of about 19°, respectively.

Although both elliptical planform configurations are unstable throughout the angle-of-attack range of the present investigation for the moment reference center used, contouring the wing lower surface causes a large reduction in stability and a positive increment in pitching-moment coefficient at zero angle of attack. The resulting pitching-moment coefficient at zero angle of attack for the ellipse (convex) model is about zero, indicating that the positive moment increment resulting from the positive pressures acting on the forward portion of the contoured wing undersurface cancels the negative pitching moment due to the fuselage nose cone.

Figure 10 compares the longitudinal aerodynamic characteristics of the trihedron model with the 75° triangular model. The trihedron model, due to both the increased frontal area and the increased effective angle of attack of the lower

surface, has larger values of drag coefficient than the 75° triangular model throughout the angle-of-attack range of the present investigation. Below an angle of attack of about 29.5°, the trihedron model also has higher values of lift coefficient than the 75° triangular model. These higher lift coefficients are attributed to the increase in effective angle of attack due to the slope of the wing lower surface. Above an angle of attack of 29.5°, the 75° triangular model develops the greater lift. The trihedron model has a value of maximum lift-drag ratio of 1.4 at an angle of attack of 11° whereas the 75° triangular model has a value of maximum lift-drag ratio of 2.3 at an angle of attack of about 14°.

As shown in figure 10, the 75° triangular model was unstable throughout the angle-of-attack range of the present investigation for the moment reference center used, but the trihedron model was stable because of its increase in volume below the assumed moment reference center.

SUMMARY OF RESULTS

An investigation has been made in the Langley 15-inch hypersonic flow apparatus to measure the static longitudinal aerodynamic characteristics of low-aspect-ratio wing-body combinations suitable for reentry. The results were obtained at a Mach number of 10.03 at angles of attack from about -4° to 42°. The Reynolds number, based on the wing mean aerodynamic chord, varied from about 0.41×10^6 to 0.58×10^6. The results of the investigation indicate the following:

1. In general, the circular planform model and the 65° triangular flat-plate model developed the highest lift coefficients and the 75° (clipped) flat-plate model developed the lowest lift coefficients throughout the angle-of-attack range.

2. Generally, for the flat-plate wing configurations, the circular model had the highest drag coefficient and the 75° clipped model had the lowest values of drag coefficient throughout the angle-of-attack range.

3. The 75° triangular configuration had the highest value of maximum lift-drag ratio (2.3) and the circular configuration had the lowest value of maximum lift-drag ratio (1.8).

4. All the flat-plate wing configurations were unstable about the wing centroid of area.

5. Changing from a semicylindrical to a square leading edge on the 65° triangular wing had essentially no effect on lift coefficient but caused higher drag, lower lift-drag ratio, and only small changes in stability.

6. Contouring the lower surface of an elliptical planform wing caused a large decrease in stability and a reduction in maximum lift-drag ratio from 2.0 to 1.4.

7. Changing from the 75° flat-plate configuration to the trihedron configuration caused a large increase in drag coefficient, a reduction in maximum lift-drag ratio from 2.3 to 1.4, and a large increase in stability. The trihedron model was the only stable configuration of the present investigation for the moment reference center used.

Langley Research Center,
National Aeronautics and Space Administration,
Langley Station, Hampton, Va., July 27, 1962.

REFERENCES

1. Foster, Gerald V.: Longitudinal Aerodynamic Characteristics at a Mach Number of 1.97 of a Series of Related Winged Reentry Configurations for Angles of Attack From 0° to 90°. NASA TM X-461, 1961.

2. Smith, Fred M., and Nichols, Frank H., Jr.: A Wind-Tunnel Investigation of the Aerodynamic Characteristics of a Generalized Series of Winged Reentry Configurations at Angles of Attack to 180° at Mach Numbers of 2.38, 2.99, and 4.00. NASA TM X-512, 1961.

3. Armstrong, William O., and Ladson, Charles L. (with appendix A by Donald L. Baradell and Thomas A. Blackstock): Effects of Variation in Body Orientation and Wing and Body Geometry on Lift-Drag Characteristics of a Series of Wing-Body Combinations at Mach Numbers From 3 to 18. NASA TM X-73, 1959

4. Wiggins, Lyle E., and Kaattari, George E.: Supersonic Aerodynamic Characteristics of Triangular Plan-Form Models at Angles of Attack to 90°. NASA TM X-568, 1961.

5. Rainey, Robert W., Fetterman, David E., Jr., and Smith, Robert: Summary of the Static Stability and Control Results of a Hypersonic Glider Investigation. NASA TM X-277, 1960.

6. Ladson, Charles L., Johnston, Patrick J., and Trescot, Charles D., Jr.: Effects of Wing Plan-Form Geometry on the Aerodynamic Characteristics of a Hypersonic Glider at Mach Numbers up to 9.6. NASA TM X-286, 1960.

TABLE I.- MODEL GEOMETRIC PARAMETERS

Model designation	A	$\bar{c}$, in.	S, sq in.	Moment center, percent $\bar{c}$
Circle	1.28	3.74	15.26	50
Ellipse	.64	5.25	15.19	49
Ellipse (convex)	.64	5.25	15.19	49
65°	1.52	3.77	14.65	50
65° (square leading edge)	1.52	3.77	14.65	50
65° (clipped)	1.16	3.99	14.75	50
75°	.96	4.75	14.33	50
Trihedron	1.13	4.64	14.56	50
75° (clipped)	.70	5.02	14.45	50

TABLE II.- SUMMARY OF AERODYNAMIC PARAMETERS

Model designation	A	C_{L_α}	$(L/D)_{max}$	$\alpha_{(L/D)max}$, deg
Circle	1.28	0.0078	1.8	22
Ellipse	.64	.0072	2.0	19
Ellipse (convex)	.64	.0088	1.4	15
65°	1.52	.0090	2.1	17
65° (square leading edge)	1.52	.0073	1.9	16
65° (clipped)	1.16	.0075	2.1	17
75°	.96	.0066	2.3	14
Trihedron	1.13	.0105	1.4	11
75° (clipped)	.70	.0065	2.2	15

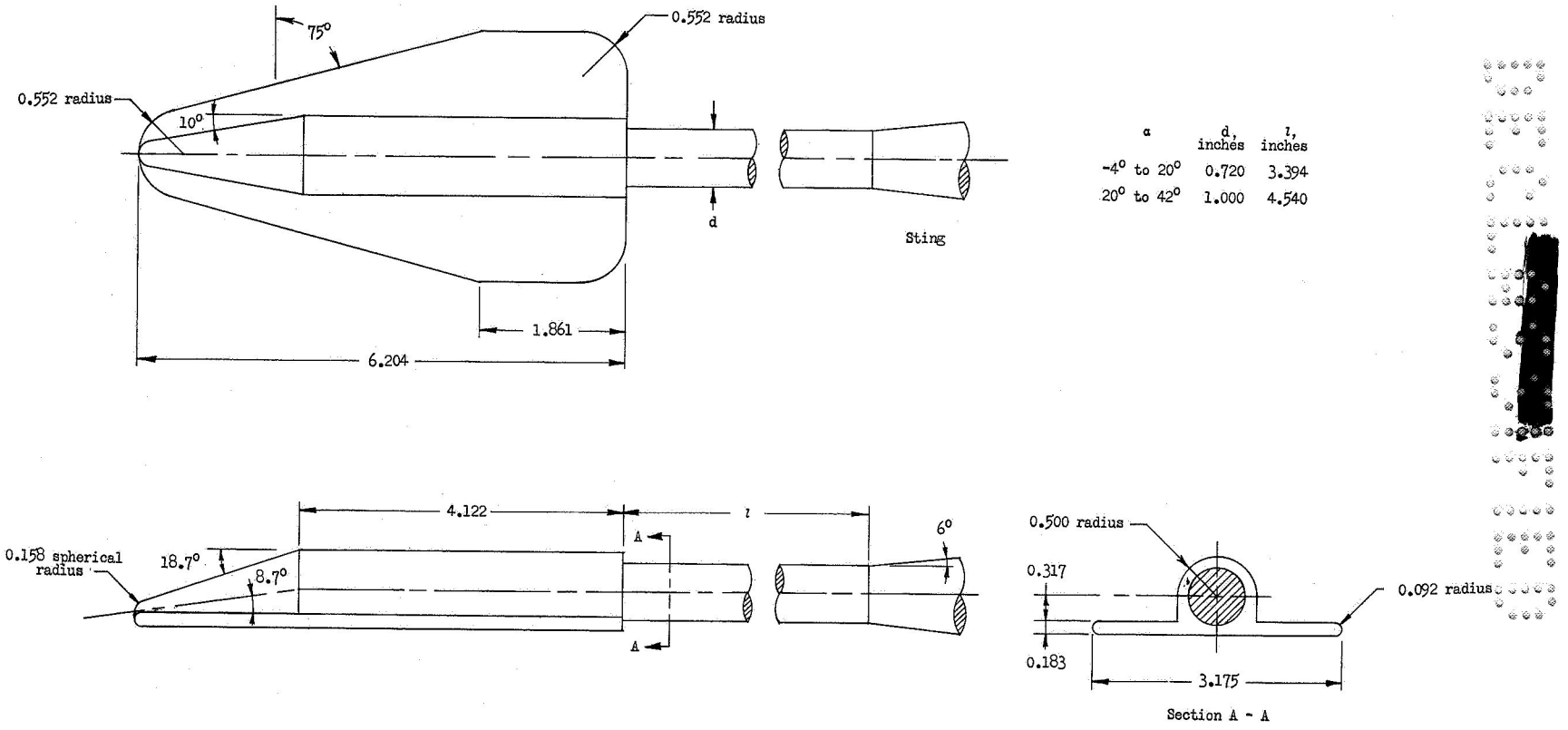

α	d, inches	l, inches
-4° to 20°	0.720	3.394
20° to 42°	1.000	4.540

Figure 1.- Typical model-sting mounting arrangment. (The 75° clipped model is shown.) All dimensions are in inches unless otherwise stated.

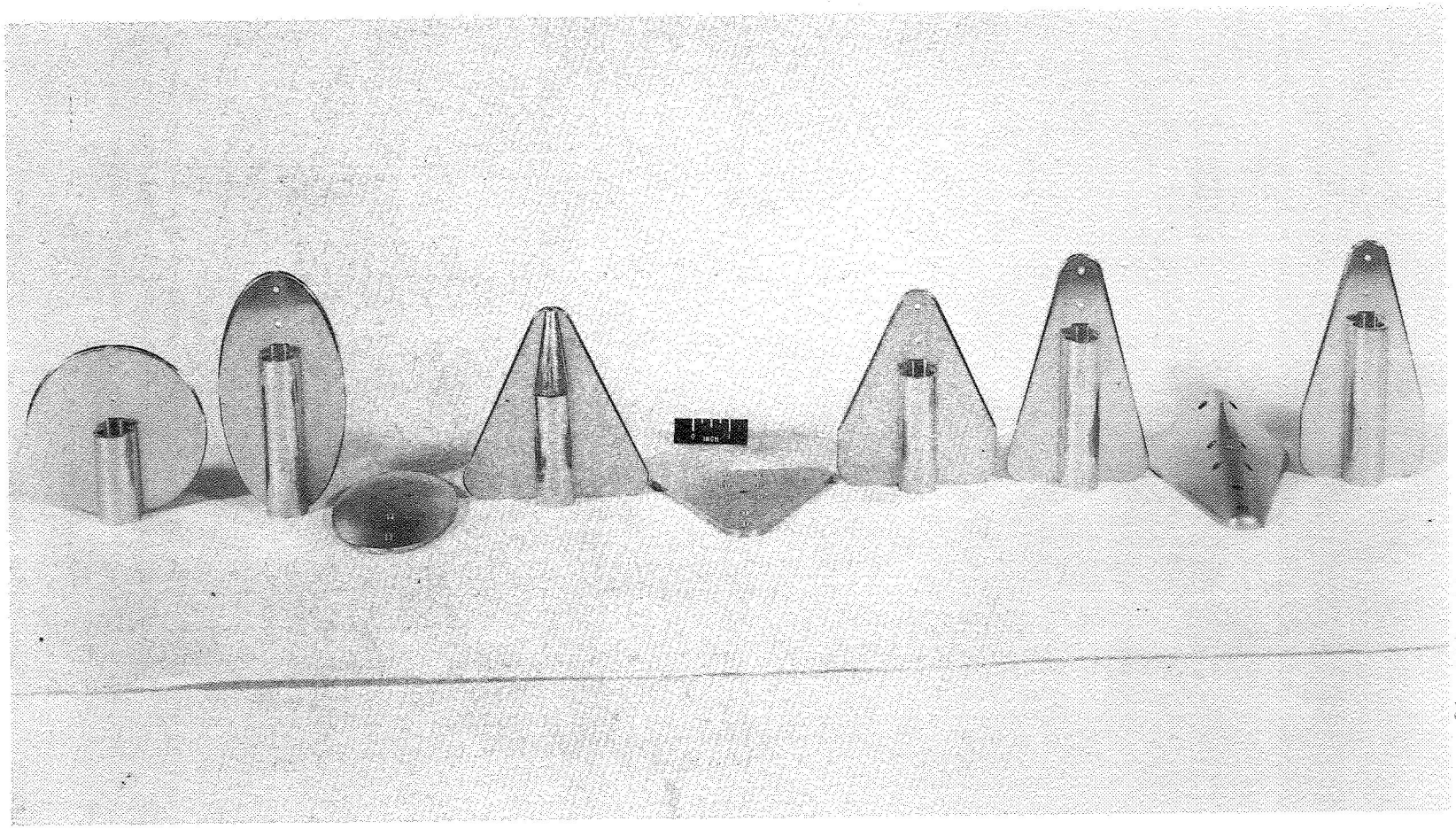

Figure 2.- Photograph of model configurations. L-59-7617

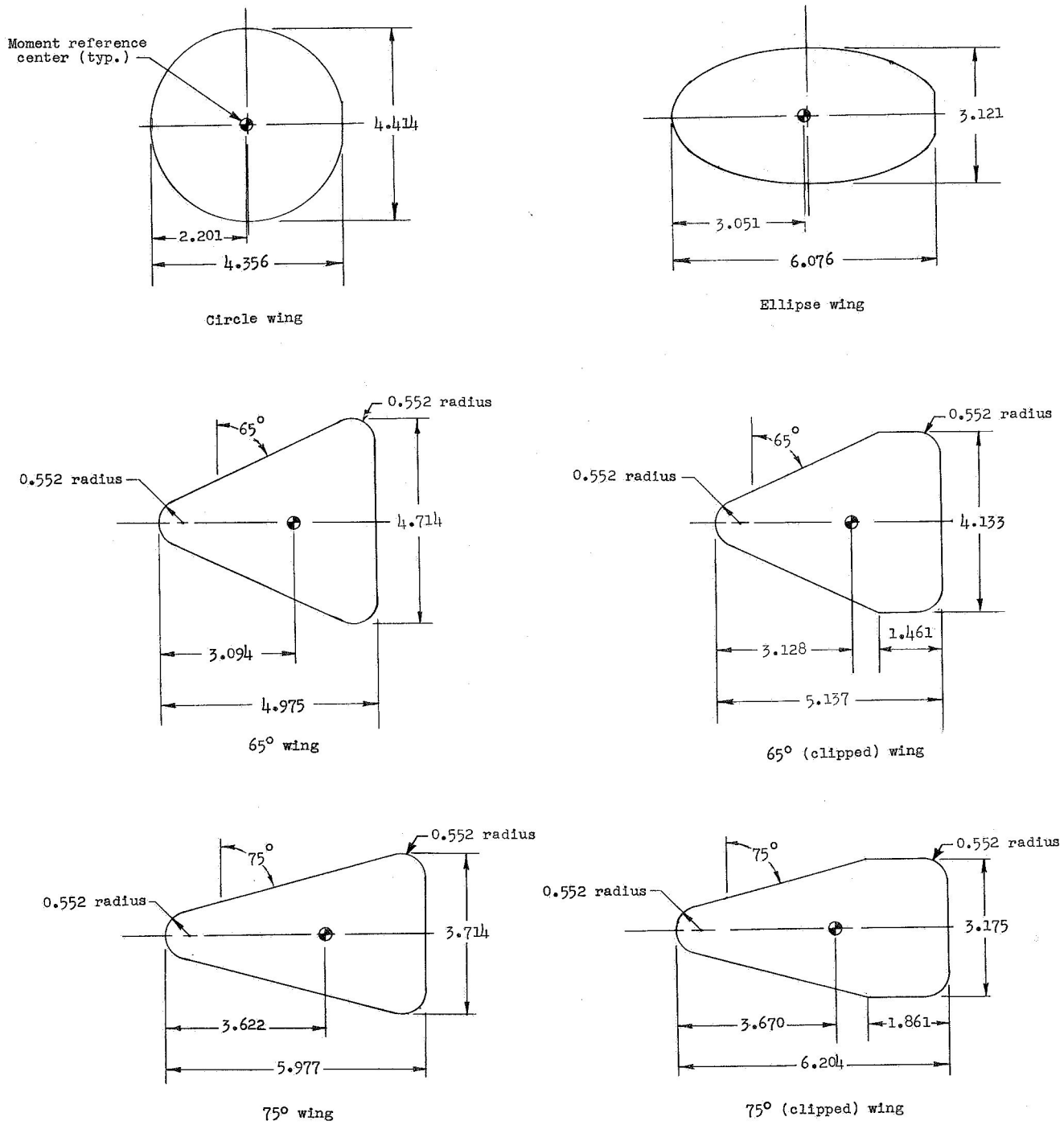

(a) Basic planform configurations.

Figure 3.- Details of the six basic flat-plate models. All dimensions are in inches unless otherwise stated.

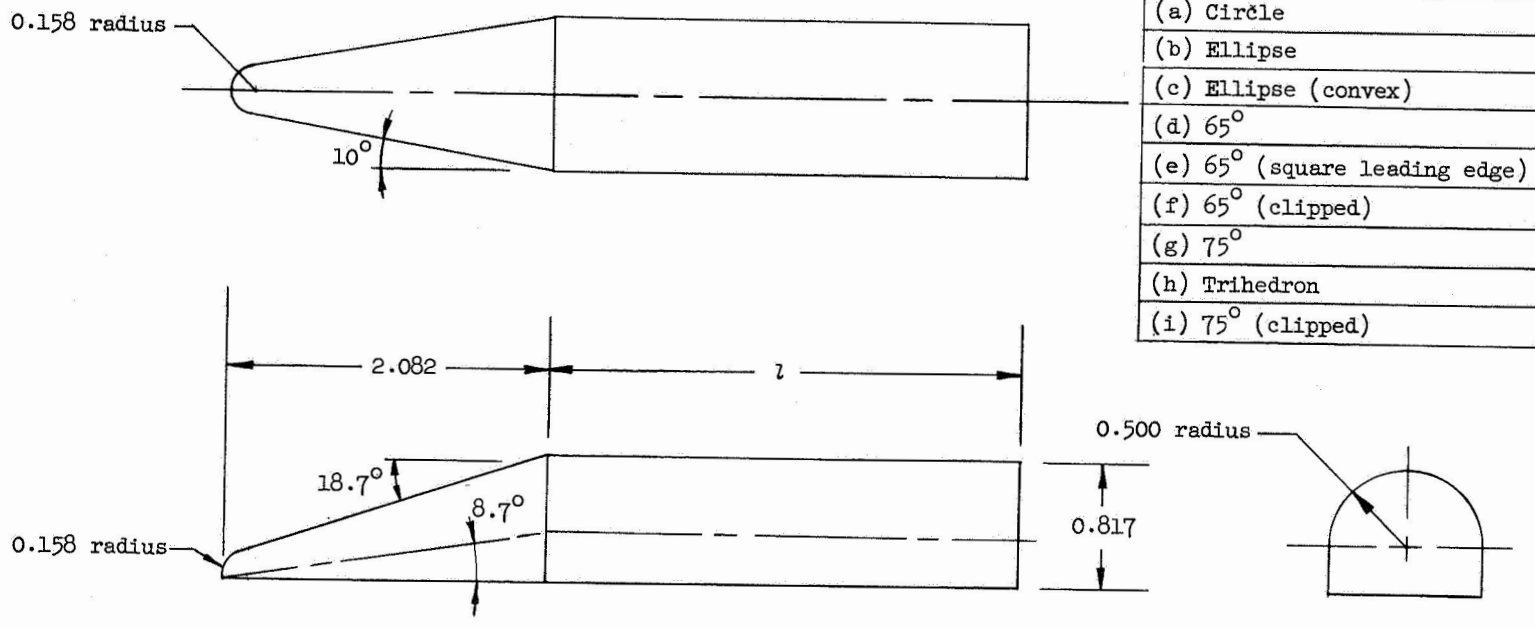

Model	l
(a) Circle	2.274
(b) Ellipse	3.994
(c) Ellipse (convex)	3.994
(d) 65°	2.893
(e) 65° (square leading edge)	2.893
(f) 65° (clipped)	3.055
(g) 75°	3.895
(h) Trihedron	3.895
(i) 75° (clipped)	4.122

(b) Body and nose drawings and dimensions.

Figure 3.- Concluded.

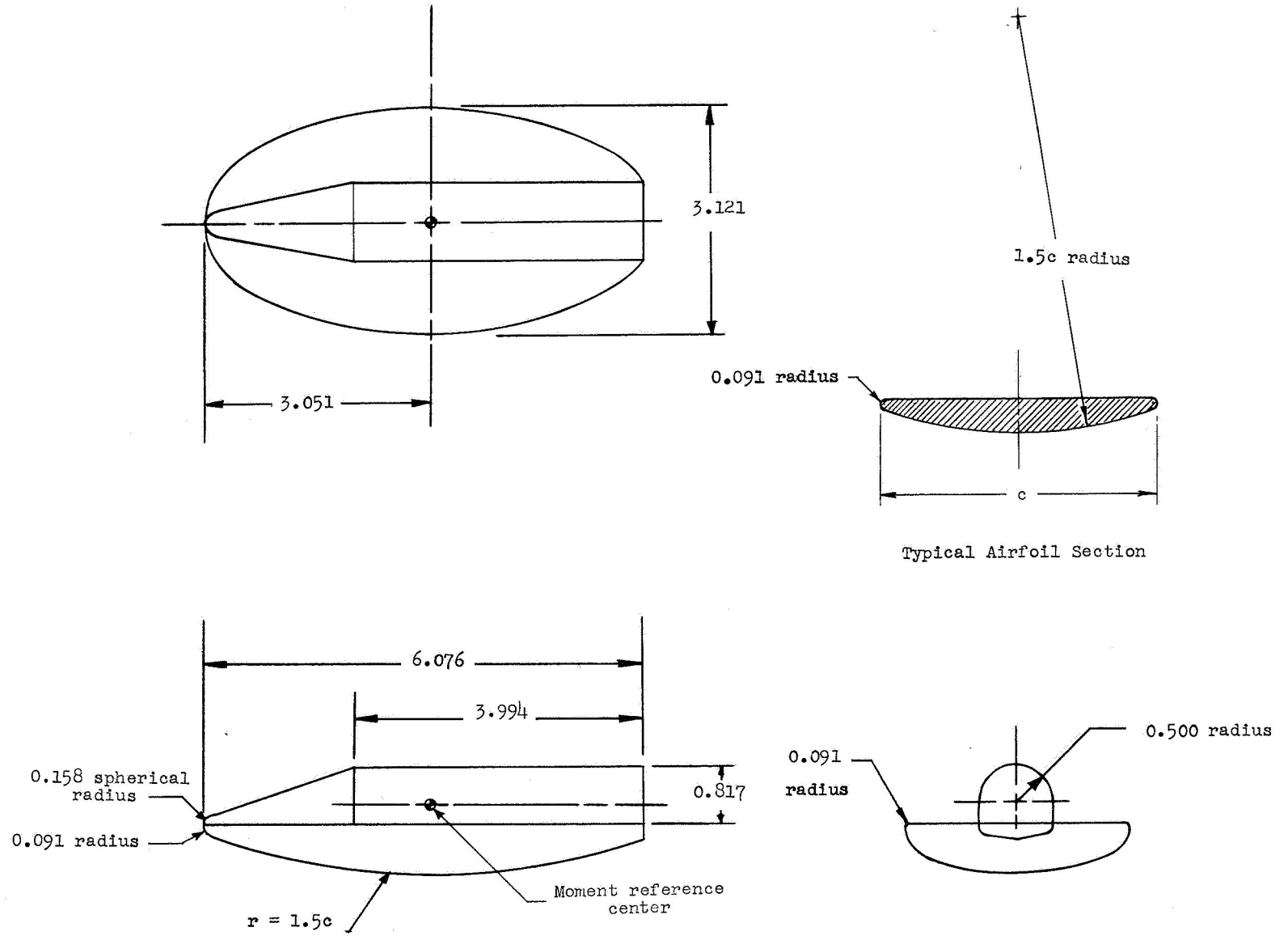

(a) Ellipse (convex) model.

Figure 4.- Drawings of the ellipse (convex) and trihedron models. All dimensions are in inches.

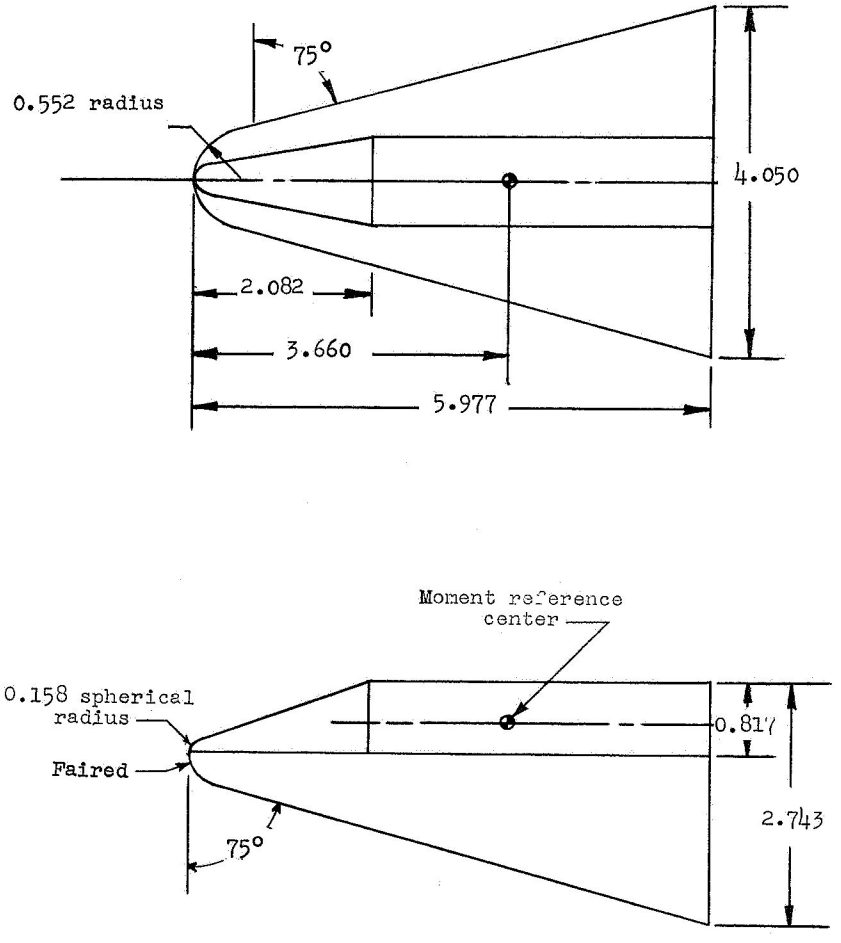

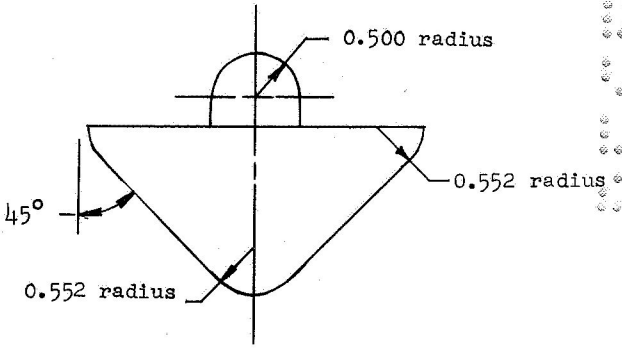

(b) Trihedron model.

Figure 4.- Concluded.

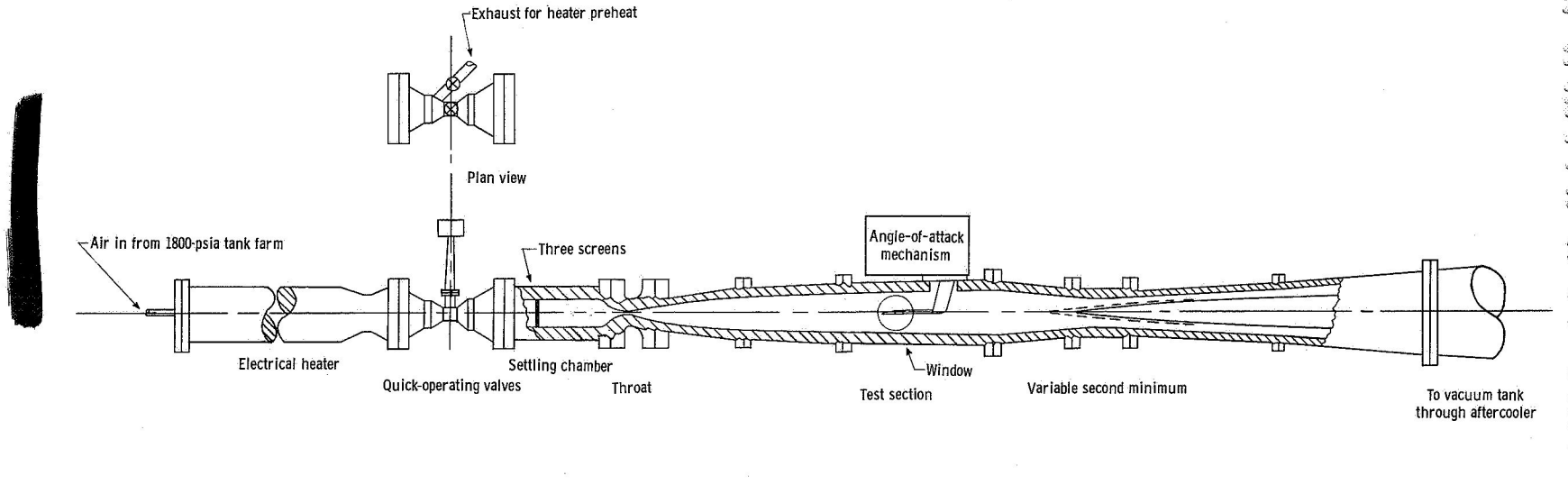

Figure 5.- Schematic drawing of the Langley 15-inch hypersonic flow apparatus.

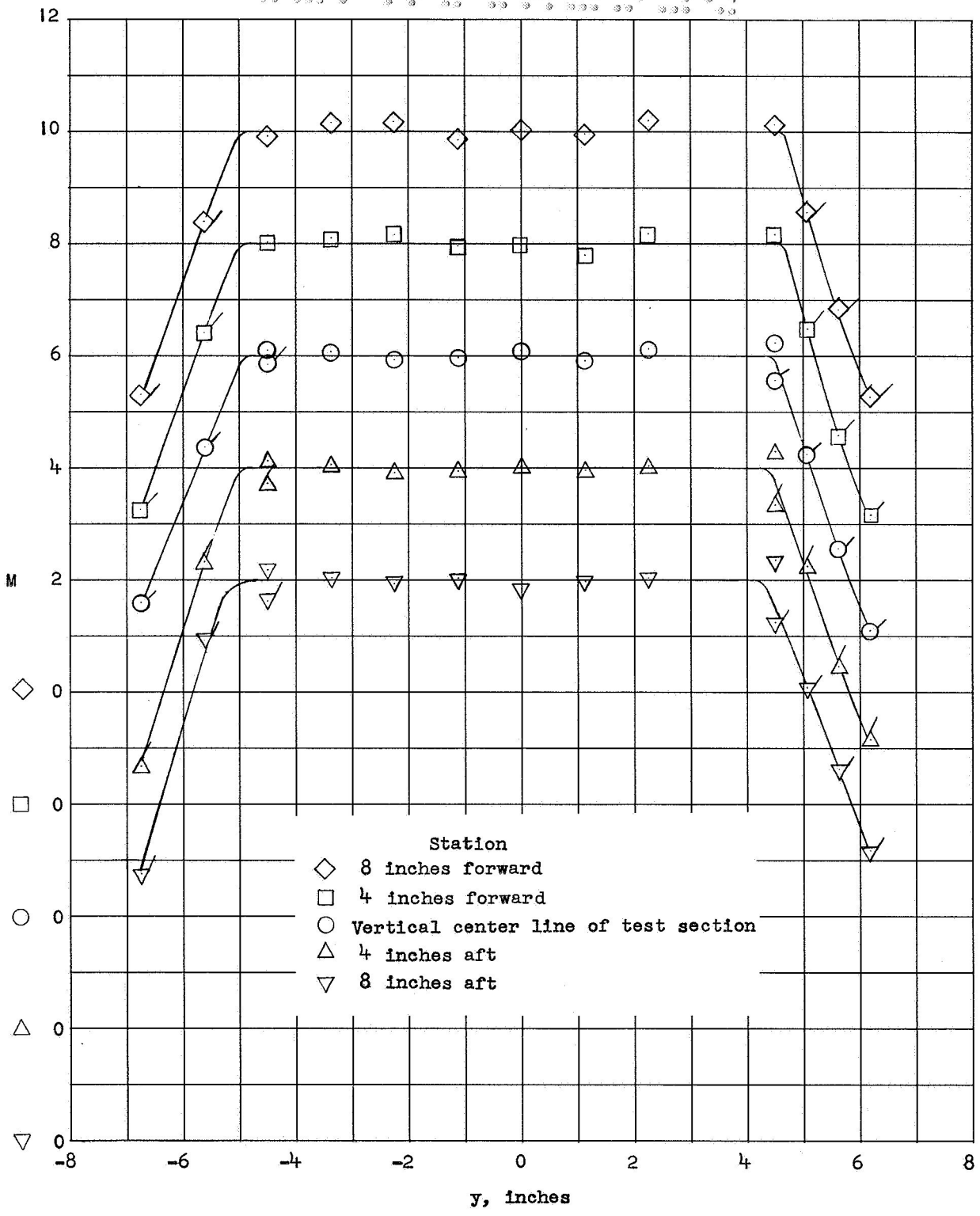

Figure 6.- Variation of Mach number with distance from tunnel horizontal center line for various longitudinal positions in the hypersonic flow apparatus. Flagged symbols denote points in the boundary layer.

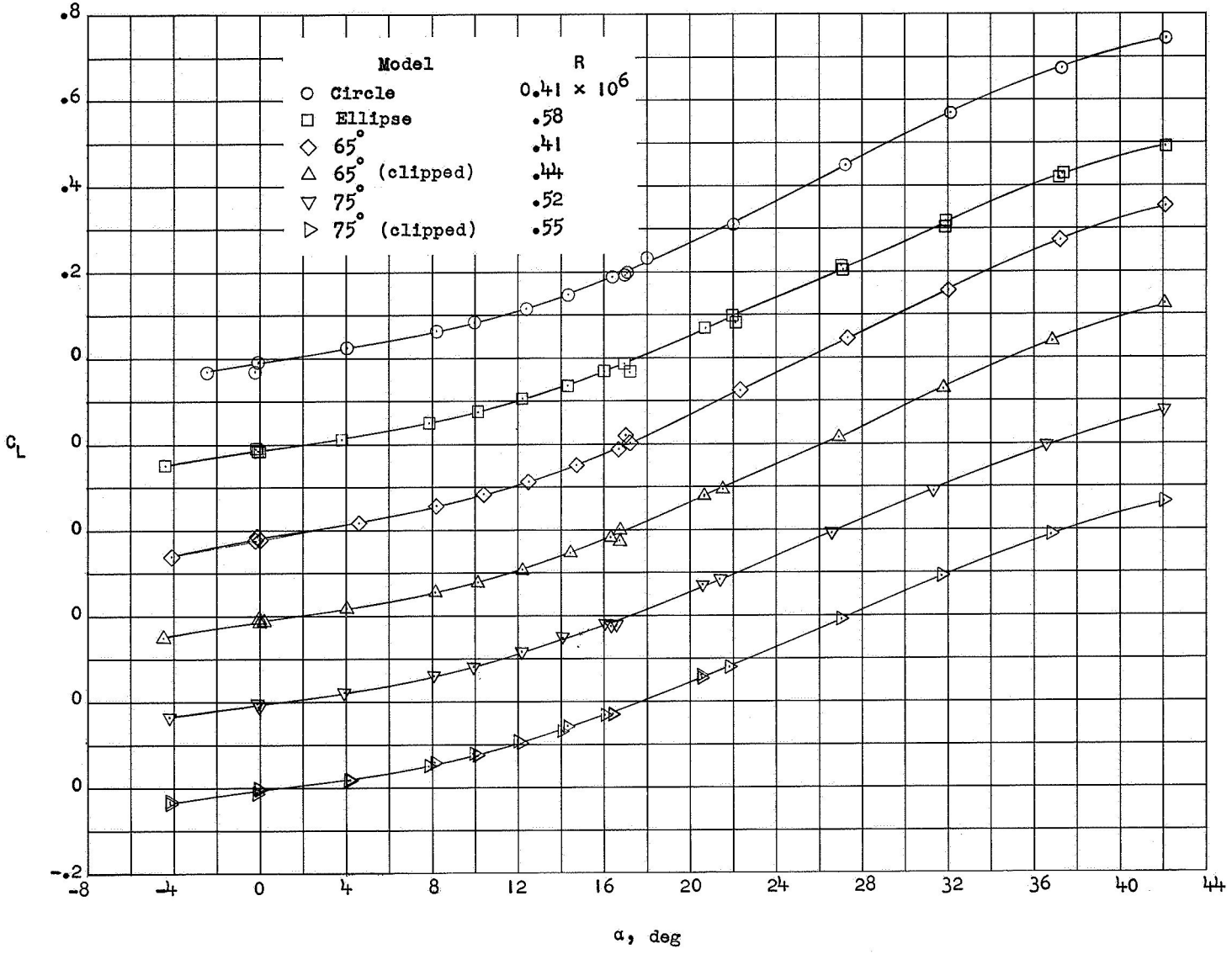

(a) Variation of C_L with α.

Figure 7.- Effect of planform variation on the longitudinal aerodynamic characteristics of flat-plate wing-body combinations at M = 10.03.

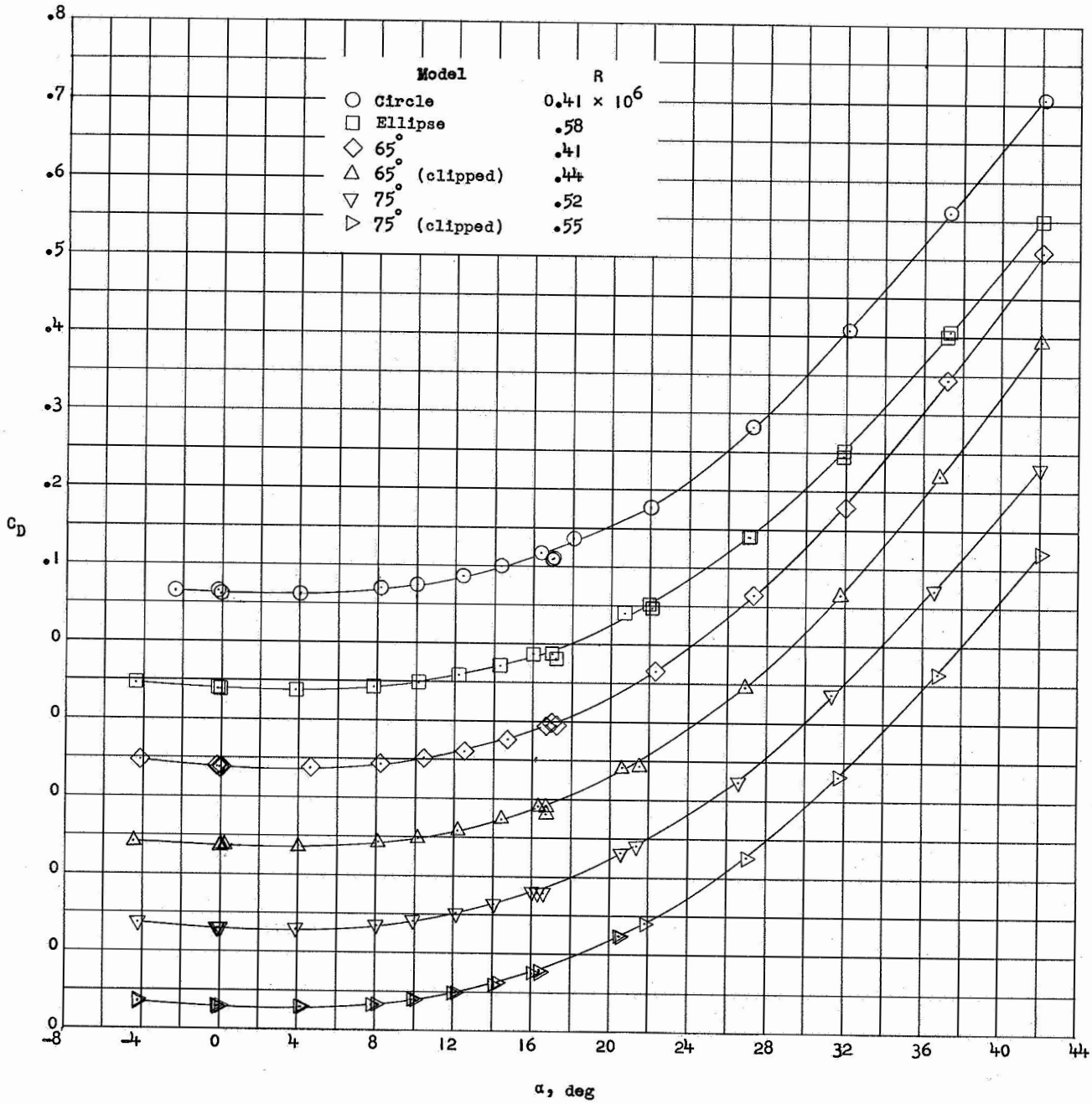

(b) Variation of C_D with α.

Figure 7.- Continued.

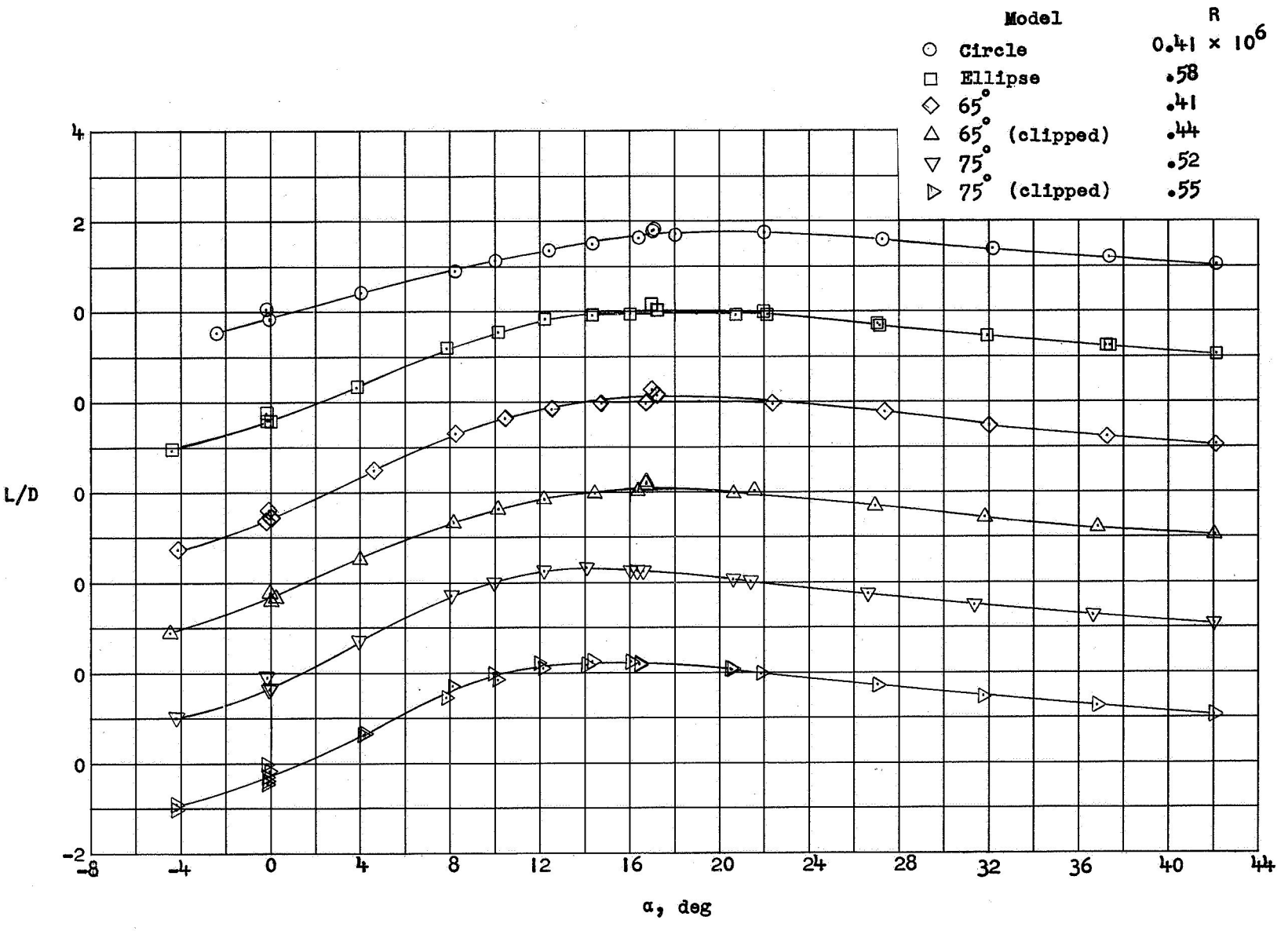

(c) Variation of L/D with α.

Figure 7.- Continued.

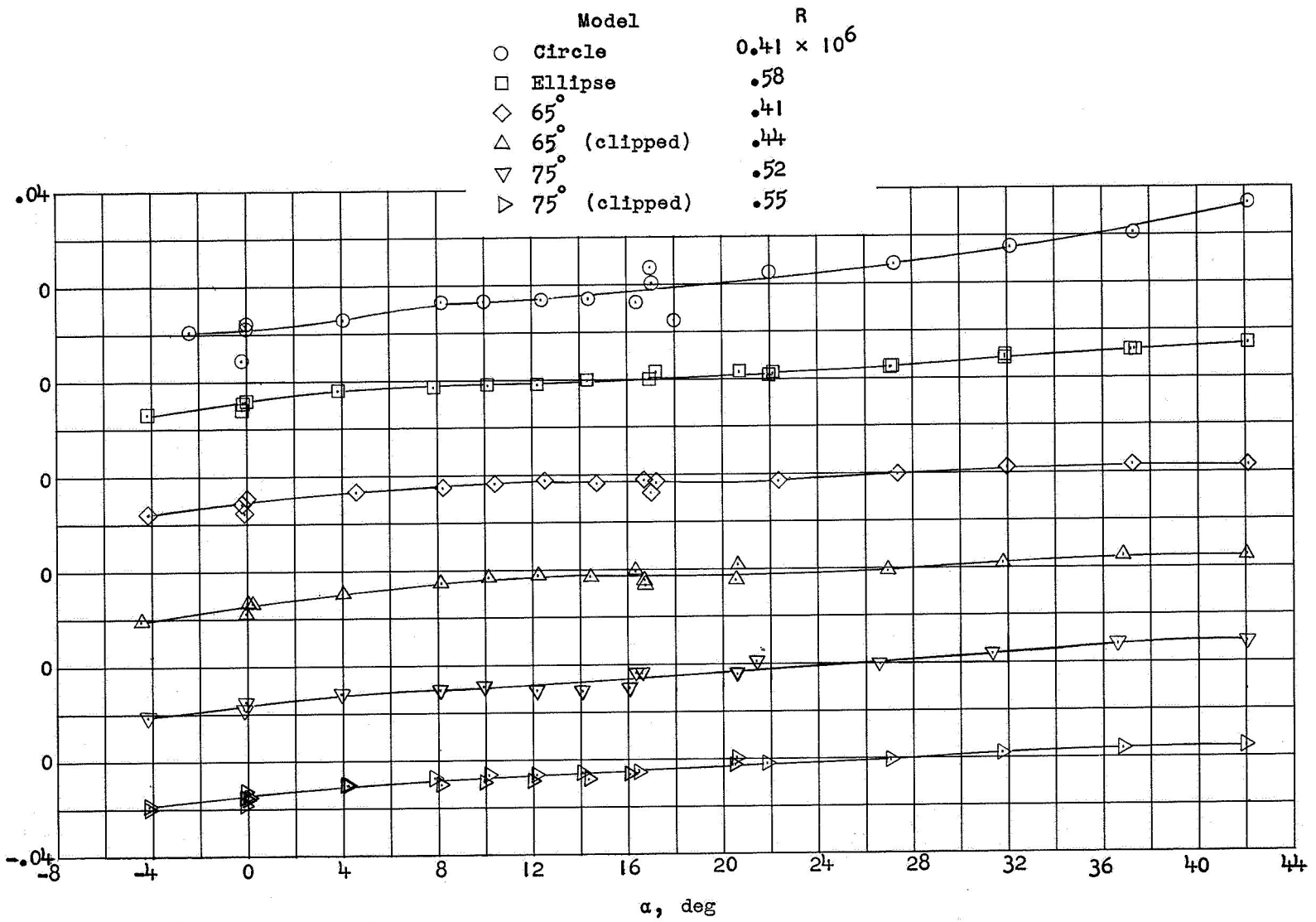

(d) Variation of C_m with α.

Figure 7.- Concluded.

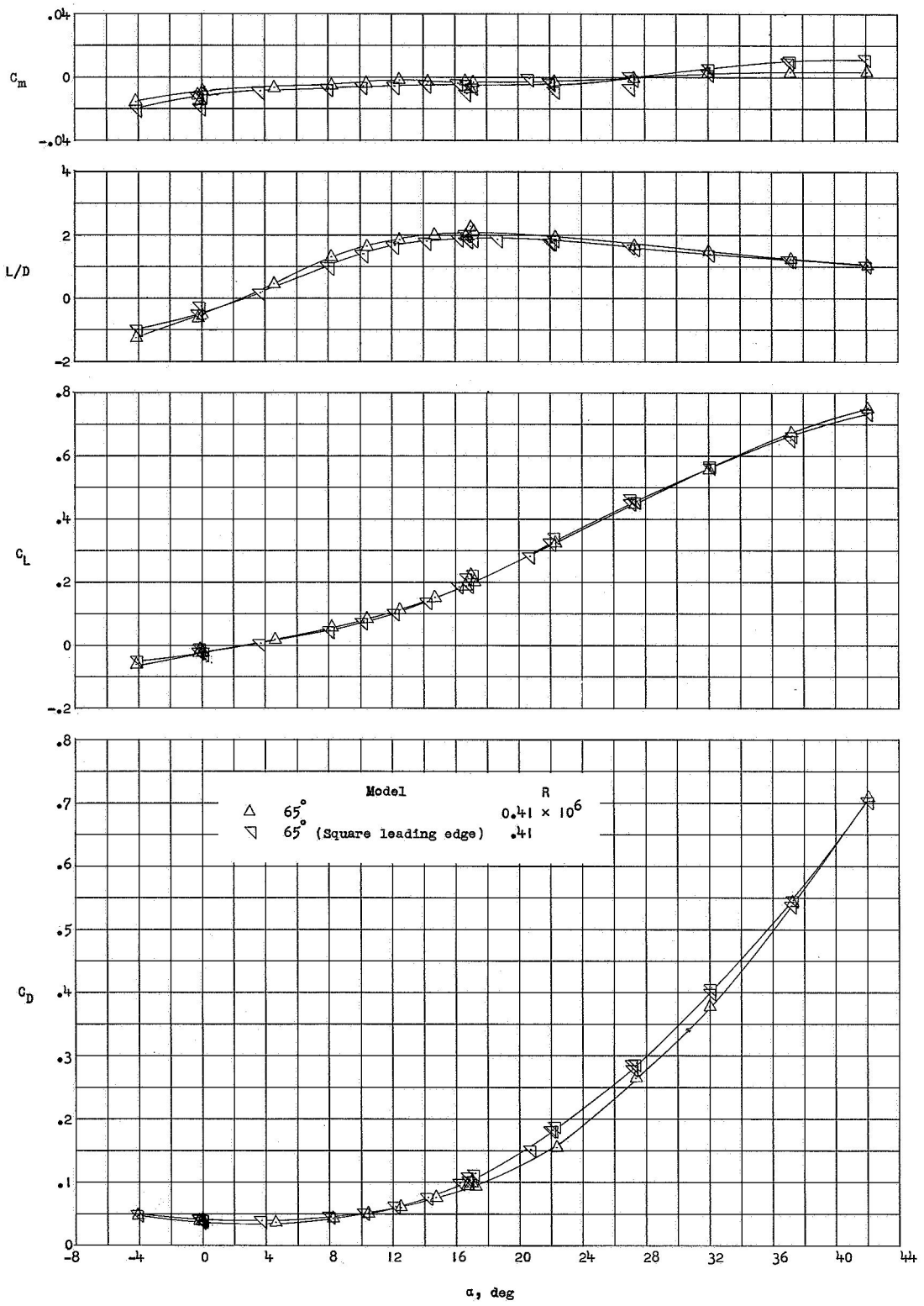

Figure 8.- Effect of wing leading-edge shape on the longitudinal aerodynamic characteristics of the 65° flat-plate configuration at M = 10.03.

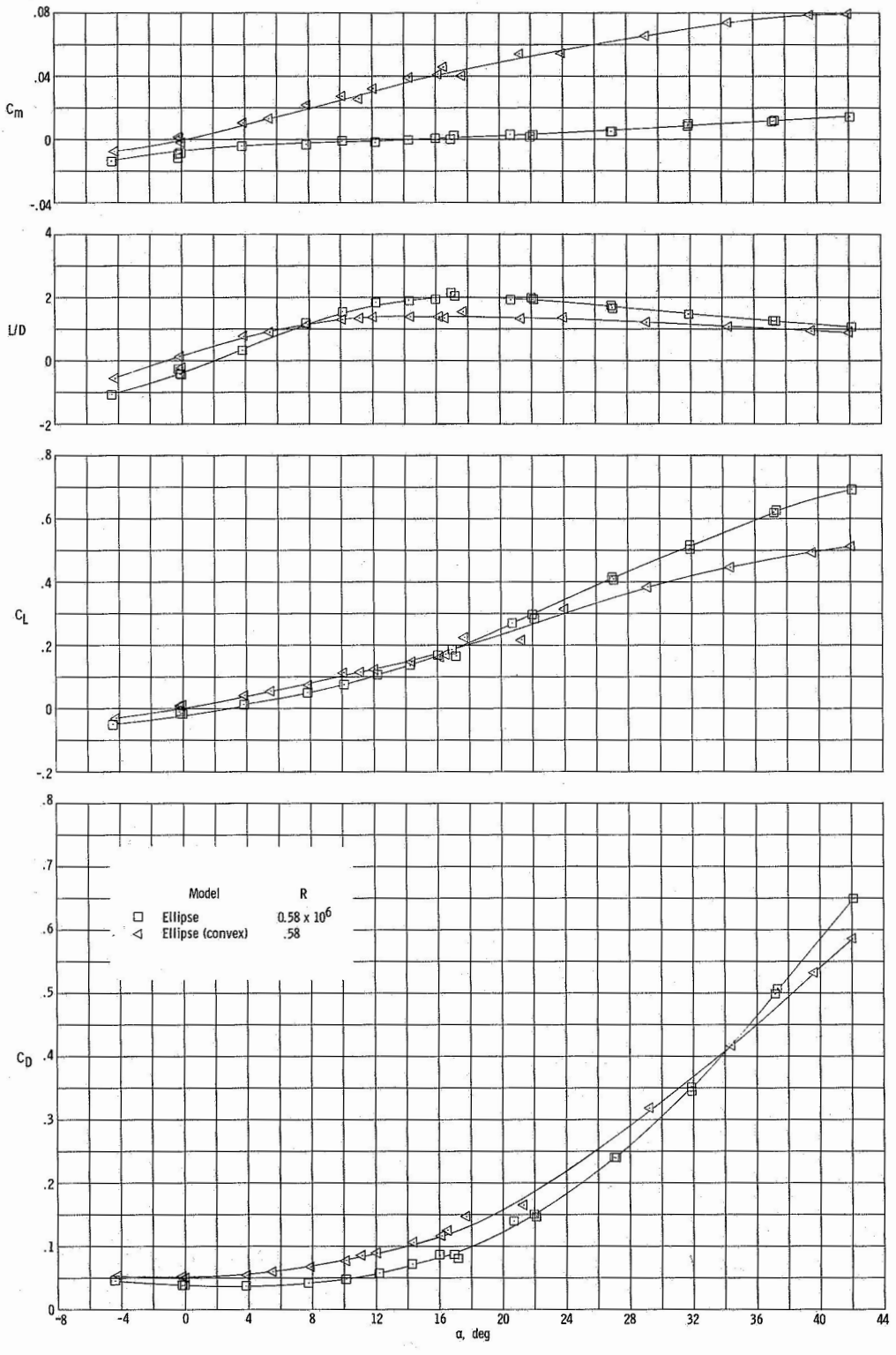

Figure 9.- Effect of lower-surface contour on the longitudinal aerodynamic characteristics of the elliptical planform configuration at M = 10.03.

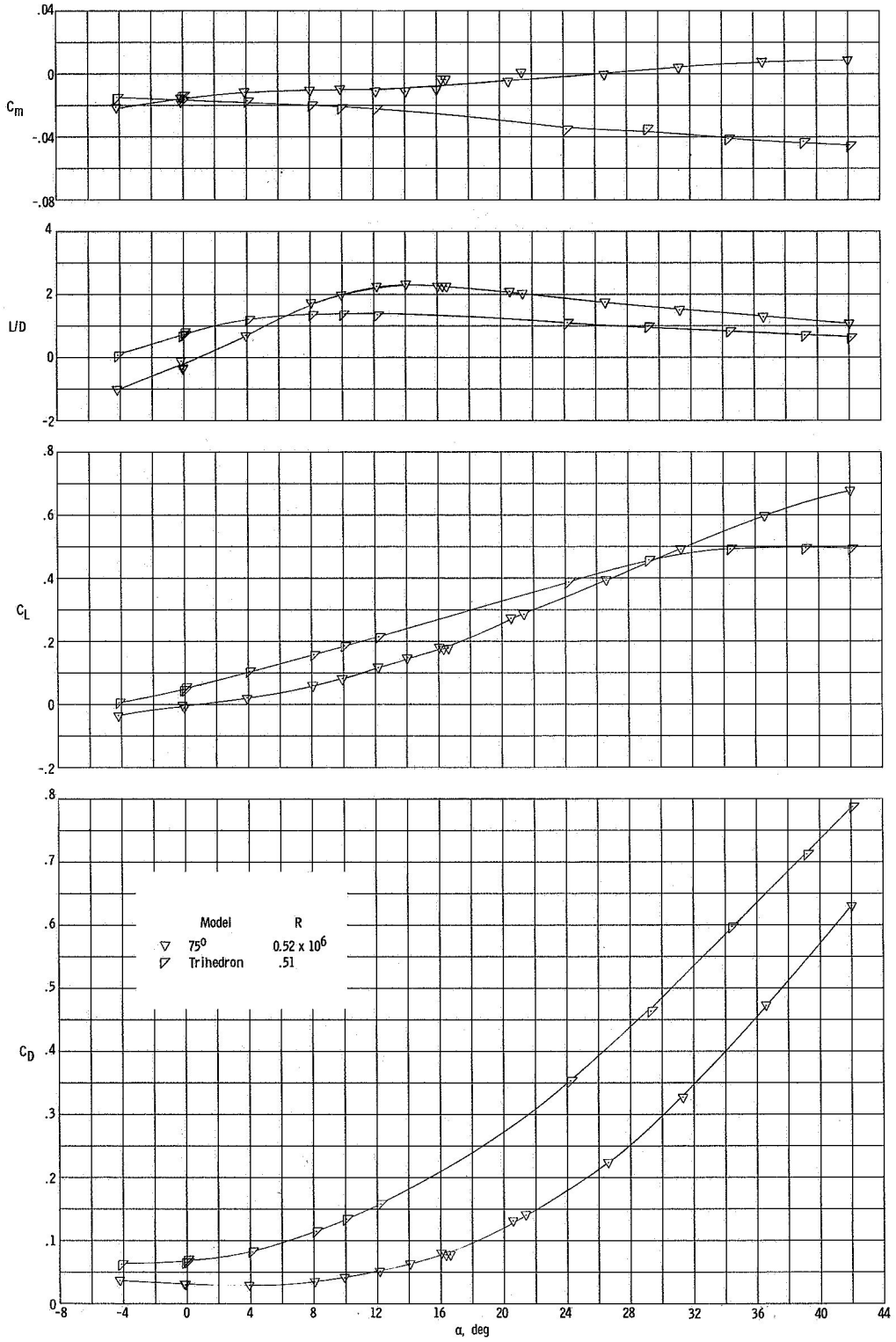

Figure 10.- Comparison of the longitudinal aerodynamic characteristics of the trihedron and the 75° triangular models at M = 10.03.

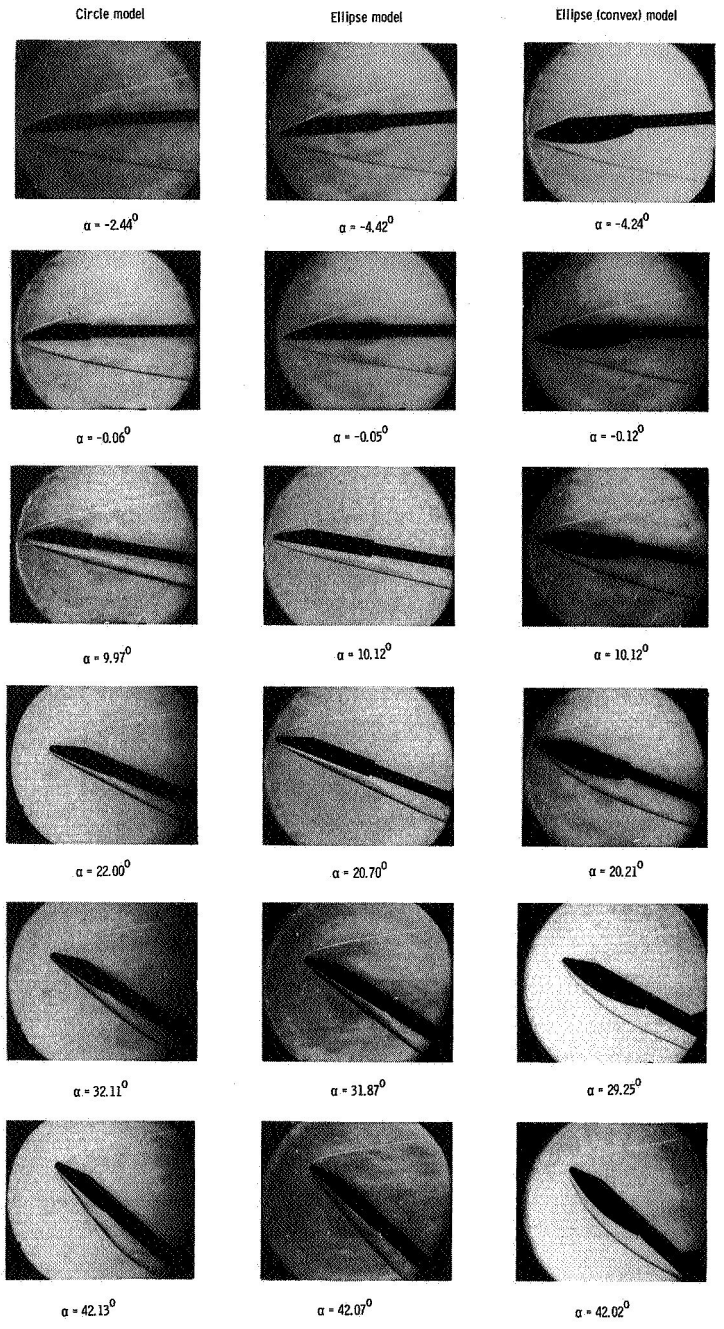

L-62-2137

(a) Circle model, ellipse model, and ellipse (convex) model.

Figure 11.- Schlieren photographs of the nine configurations at angles of attack near $\alpha = -4^\circ, 0^\circ, 10^\circ, 20^\circ, 30^\circ$, and 40°.

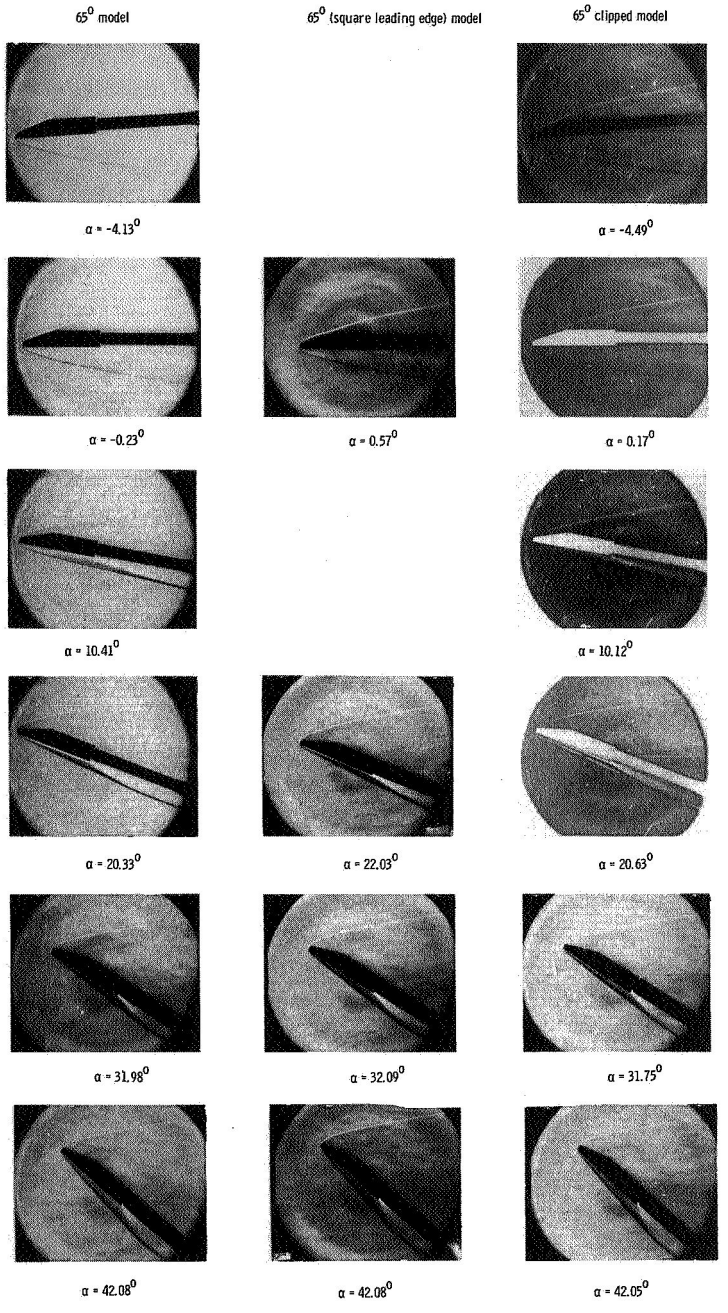

L-62-2138

(b) 65° model, 65° (square leading edge) model, and 65° clipped model.

Figure 11.- Continued.

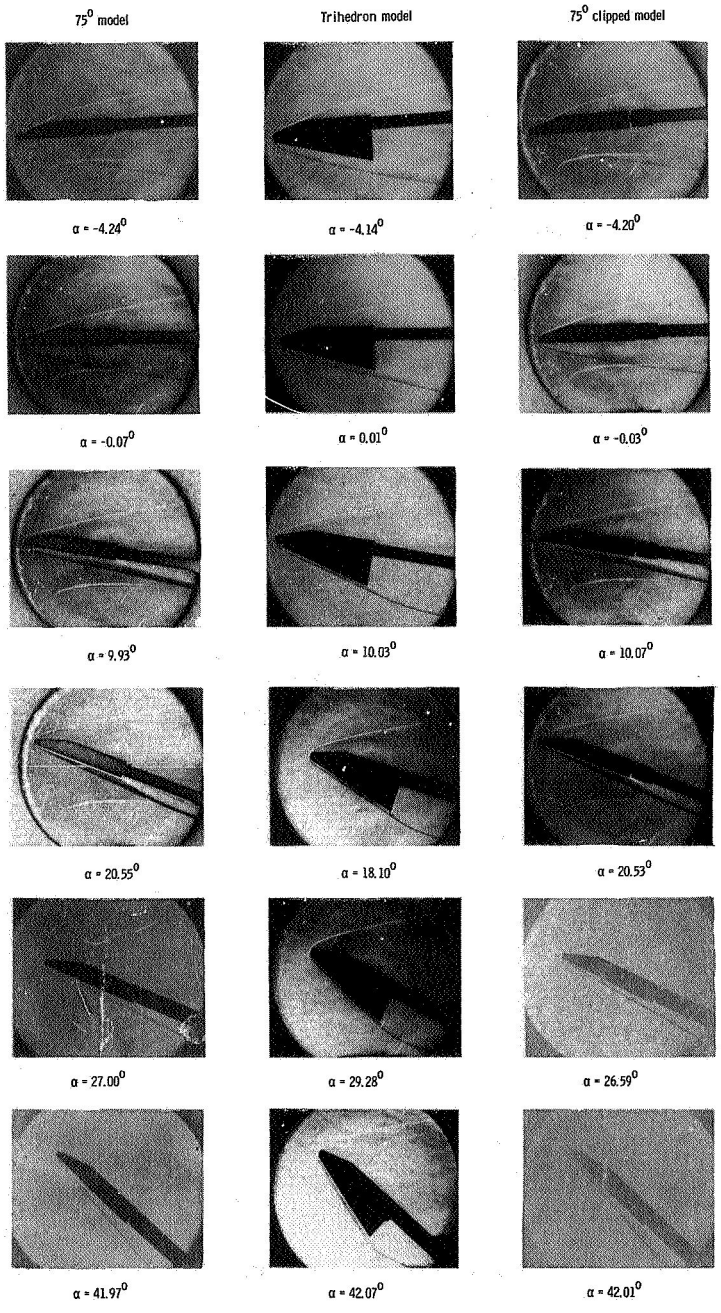

L-62-2139

(c) 75° model, trihedron model, and 75° clipped model.

Figure 11.- Concluded.

NASA-Langley, 1962 L-1893